Mimetic finite elements

Mimetic properties

Discrete versions of calculus identities:
$\nabla\cdot\nabla^\perp\psi = 0$, $\nabla^\perp\cdot\nabla D = 0$, $\nabla^\perp\cdot\boldsymbol{u}^\perp = \nabla\cdot\boldsymbol{u}$, where $(\nabla^\perp = \boldsymbol{k}\times\nabla)$.

Compatible finite element spaces in 2D

$$\underbrace{\mathbb{V}_0}_{\text{Continuous}} \xrightarrow{\nabla^\perp=(-\partial_y,\partial_x)} \underbrace{\mathbb{V}_1}_{\text{Continuous normals}} \xrightarrow{\nabla\cdot} \underbrace{\mathbb{V}_2}_{\text{Discontinuous}}$$

- $\nabla\cdot$ maps from $\mathbb{V}_1$ onto $\mathbb{V}_2$.
- $\nabla^\perp$ maps from $\mathbb{V}_0$ onto $\ker(\nabla\cdot)$ in $\mathbb{V}_1$.

Applied to the linearised shallow water equations:

1) global energy conservation 2) local mass conservation
3) steady geostrophic states 4) no spurious pressure modes

Application to nonlinear shallow water equations

$$\boldsymbol{u}_t + (\underbrace{\boldsymbol{u}qD}_{\boldsymbol{Q}})^{\perp} = -\nabla\left(\frac{1}{2}|\boldsymbol{u}|^2 + gD\right) \quad (1) \qquad D_t + \nabla(\underbrace{\boldsymbol{u}D}_{\boldsymbol{F}}) = 0 \quad (2)$$

where $q = \frac{\zeta+f}{D}$ and $\zeta = \nabla^{\perp}\boldsymbol{u}$

$\nabla^{\perp}(1)$ gives $$(qD)_t + \nabla\cdot\boldsymbol{Q} = 0 \quad (3)$$

Timestepping:

- within each timestep perform multiple quasi Newton iterations: solve the Helmholtz equation for updates to $\boldsymbol{u}$ and D using a hybridized method
- first need to calculate $\boldsymbol{F}$ and $\boldsymbol{Q}$:
  - solve equation 2 for D and calculate mass flux $\boldsymbol{F}$: flux reconstruction
  - solve equation 3 for q and diagnose potential vorticity flux $\boldsymbol{Q}$: Taylor-Galerkin methods

Mimetic finite element methods for solving the nonlinear rotating shallow water equations.

Jemma Shipton and Colin Cotter

Department of Mathematics, Imperial College London

Imperial College London

NERC SCIENCE OF THE ENVIRONMENT

Motivation

- Construct numerical schemes that have all the desirable properties of the C-grid finite difference discretisation, without the constraint that the grid be orthogonal
- Devise stable, consistent advection schemes for both layer depth (discontinuous) and potential vorticity (continuous) fields
- Present benchmarking results from standard testcases

Mimetic properties

Discrete analogues of the vector calculus identities

$$\nabla\cdot\nabla^{\perp}\psi\equiv 0,\quad \nabla^{\perp}\cdot\nabla\psi\equiv 0,\quad \nabla^{\perp}\cdot\boldsymbol{u}^{\perp}\equiv\nabla\cdot\boldsymbol{u}$$

where $\nabla^{\perp}=\boldsymbol{k}\times\nabla$ and $\boldsymbol{u}^{\perp}=\boldsymbol{k}\times\boldsymbol{u}$ where $\boldsymbol{k}$ is the normal to the surface.
Applied to the linearised shallow water equations [1]:

- satisfy LBB condition
- global energy conservation
- local mass conservation
- steady geostrophic modes
- no spurious pressure modes

Shallow water equations

$$\boldsymbol{u}_t+(\zeta+f)\boldsymbol{u}^{\perp}+\nabla\left(g(D+b)+\frac{1}{2}|\boldsymbol{u}|^2\right)=0 \quad (1) \qquad D_t+\nabla\cdot(\boldsymbol{u}D)=0 \quad (2)$$

$\boldsymbol{u}$: horizontal velocity, D: layer depth, b: height of the lower boundary, f: Coriolis parameter, ζ: vorticity ($=\nabla^{\perp}\boldsymbol{u}$), g: gravitational acceleration.
Combining equation 2 with $\nabla^{\perp}$ equation 1 gives Lagrangian conservation of potential vorticity, q:

$$q_t+(\boldsymbol{u}\cdot\nabla)q=0,\quad \text{where}\quad q=\frac{\zeta+f}{D}$$

Compatible finite element spaces

$$\begin{array}{ccccc} H^1 & \xrightarrow{\nabla^{\perp}} & H(\mathrm{div}) & \xrightarrow{\nabla\cdot} & L^2 \\ \downarrow{\scriptstyle \pi_0} & & \downarrow{\scriptstyle \pi_1} & & \downarrow{\scriptstyle \pi_2} \\ \mathbb{V}_0 & \xrightarrow{\nabla^{\perp}} & \mathbb{V}_1 & \xrightarrow{\nabla\cdot} & \mathbb{V}_2 \end{array}$$

- The condition that $\boldsymbol{u}\in\mathbb{V}_1\subset H(\mathrm{div})$ means that $\boldsymbol{u}$ must have continuous normal components.
- $D\in\mathbb{V}_2$ is fully discontinuous.

$$\underbrace{\mathbb{V}_0=P2+}_{\text{Quadratic (+1 Cubic) Continuous}} \xrightarrow{\nabla^{\perp}} \underbrace{\mathbb{V}_1=BDFM1}_{\text{Linear (+2 Quadratic) Cont. normals}} \xrightarrow{\nabla\cdot} \underbrace{\mathbb{V}_2=P1_{DG}}_{\text{Linear Discontinuous}}$$

$$\underbrace{\mathbb{V}_0=Q2}_{\text{Biquadratic Continuous}} \xrightarrow{\nabla^{\perp}} \underbrace{\mathbb{V}_1=RT1}_{\text{Bilinear/Biquadratic, Cont. normals}} \xrightarrow{\nabla\cdot} \underbrace{\mathbb{V}_2=Q1_{DG}}_{\text{Bilinear, Discontinuous}}$$

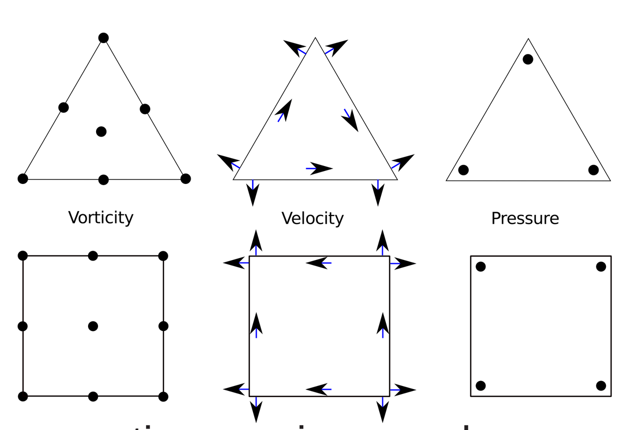

Both satisfy $\dim(\mathbb{V}_1)=2\dim(\mathbb{V}_2)$, the condition necessary for preventing spurious modes.

Constructing $\mathbb{V}_1$ on the sphere

Integrals are computed over a reference element so we need to map to the physical element

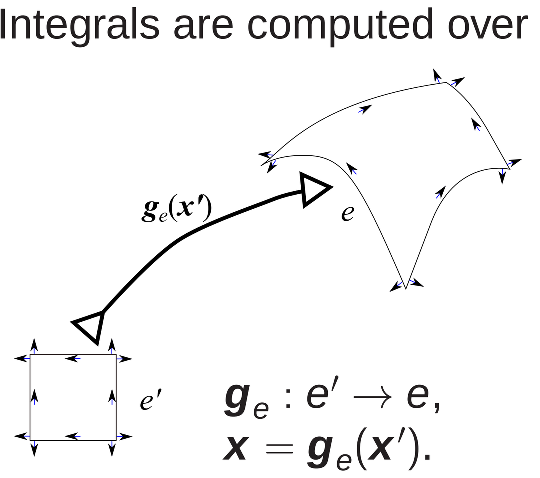

$$\boldsymbol{g}_e: e'\to e,\qquad \boldsymbol{x}=\boldsymbol{g}_e(\boldsymbol{x}').$$

For vector fields we use the Piola transformation $\boldsymbol{u}'\mapsto\boldsymbol{u}$:

$$\boldsymbol{u}(\boldsymbol{g}_e(\boldsymbol{x}'))=\frac{J\boldsymbol{u}'}{\det J},\quad \text{where}\quad J=\frac{\partial\boldsymbol{g}_e}{\partial\boldsymbol{x}'}$$

- Ensures $\boldsymbol{u}$ is tangent to the surface of the sphere
- Divergence:
$$\nabla\cdot\boldsymbol{u}(\boldsymbol{g}(\boldsymbol{x}'))=\frac{\nabla'\cdot\boldsymbol{u}'(\boldsymbol{x}')}{\det J(\boldsymbol{x}')}.$$
- Normal components:
$$\int_f\boldsymbol{u}'\cdot\boldsymbol{n}'\,\mathrm{d}x=\int_{\boldsymbol{g}_e(f)}\boldsymbol{u}\cdot\boldsymbol{n}\,\mathrm{d}x.$$

All matrices (except mass matrices) are topological, i.e. they are independent of coordinates.

Mixed finite element discretisation

Multiply equations 1-2 by appropriate test functions, $\boldsymbol{w}\in\mathbb{V}_1$ and $\phi\in\mathbb{V}_2$, and integrate over the domain Ω:

$$\int_\Omega\boldsymbol{w}\cdot\boldsymbol{u}_t\,\mathrm{d}V+\int_\Omega\boldsymbol{w}\cdot\boldsymbol{Q}^{\perp}\,\mathrm{d}V-\int_\Omega\nabla\cdot\boldsymbol{w}\left(g(D+b)+\frac{1}{2}|\boldsymbol{u}|^2\right)\mathrm{d}V=0, \qquad (3)$$

$$\int_\Omega\phi\,(D_t+\nabla\cdot\boldsymbol{F})\,\mathrm{d}V=0, \qquad (4)$$

where we have introduced the mass flux $\boldsymbol{F}=\boldsymbol{u}D$ and potential vorticity flux $\boldsymbol{Q}=q\boldsymbol{F}$. Require discrete potential vorticity $q\in\mathbb{V}_0$ to satisfy

$$\int_\Omega\gamma qD\,\mathrm{d}V=\int_\Omega-\nabla^{\perp}\gamma\boldsymbol{u}\,\mathrm{d}V+\int_\Omega\gamma f\,\mathrm{d}V\quad\forall\gamma\in\mathbb{V}_0. \qquad (5)$$

Differentiate equation 5 and substitute for $\boldsymbol{u}_t$ using equation 3 with $\boldsymbol{w}=-\nabla^{\perp}\gamma$. Since $\nabla\cdot\nabla^{\perp}\equiv 0$ and we assume $f_t=0$, this gives an advection equation for q:

$$\int_\Omega\gamma(qD)_t+\nabla\gamma\cdot\boldsymbol{Q}\,\mathrm{d}V=0. \qquad (6)$$

Rearranging gives:

$$\int_\Omega\gamma(Dq_t+\boldsymbol{F}\cdot\nabla q)\,\mathrm{d}V=-\int_\Omega\gamma q\underbrace{(D_t+\nabla\cdot\boldsymbol{F})}_{=0\text{for flat elements [3]}}\,\mathrm{d}V. \qquad (7)$$

i.e. if q is initially spatially constant it will remain so. This consistency can be recovered for higher order curved elements (see Colin's talk).

Timestepping

- discretise equations 3-4 in time using the theta method
- within each timestep perform multiple quasi Newton iterations: solve the Helmholtz equation for updates to $\boldsymbol{u}$ and D (see following box)
- first need to calculate $\boldsymbol{F}$ and $\boldsymbol{Q}$:
  - solve equation 4 for D and calculate mass flux $\boldsymbol{F}$ (see flux reconstruction)
  - solve equation 6 for q and diagnose potential vorticity flux $\boldsymbol{Q}$ (see Taylor-Galerkin methods)

Hybridized Helmholtz equation

$$\int_\Omega\boldsymbol{w}\cdot\Delta\boldsymbol{u}\,\mathrm{d}x-\Delta t\int_\Omega\nabla\cdot\boldsymbol{w}\Delta D\,\mathrm{d}x=\int_\Omega\boldsymbol{w}\cdot R_{\boldsymbol{u}}\,\mathrm{d}x\quad\forall\boldsymbol{w}\in\mathbb{V}_1$$

$$\int_\Omega\phi\Delta D\,\mathrm{d}x+\Delta t\int_\Omega\phi\nabla\cdot\boldsymbol{u}\,\mathrm{d}x=\int_\Omega\phi R_D\,\mathrm{d}x\quad\forall\phi\in\mathbb{V}_2$$

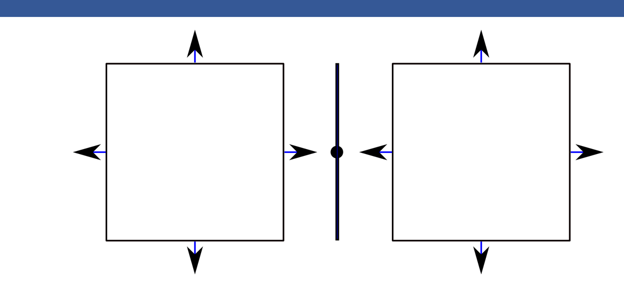

Trace space for RT0 elements

- Relax continuity constraints and allow $\boldsymbol{u}$ to be fully discontinuous
- Define a set of Lagrange multipliers $\boldsymbol{\lambda}$ on the trace space of $\mathbb{V}_1$ (i.e. on the set of element edges) and use these to enforce continuity of the normal component of $\boldsymbol{u}$.
$$\int_\Gamma\mu[\boldsymbol{u}\cdot\boldsymbol{n}]ds=0,\ \int_\Omega\bar{\boldsymbol{w}}\cdot\Delta\bar{\boldsymbol{u}}\,\mathrm{d}x-\Delta t\int_\Omega\nabla\cdot\bar{\boldsymbol{w}}\Delta D\,\mathrm{d}x=\int_\Omega\bar{\boldsymbol{w}}\cdot R_{\boldsymbol{u}}\,\mathrm{d}x+\int_\Gamma\lambda[\boldsymbol{w}\cdot\boldsymbol{n}]\,\mathrm{d}s\quad\forall\bar{\boldsymbol{w}}\in\bar{\mathbb{V}}_1$$
- Eliminate both $\boldsymbol{u}$ and D to give a *symmetric, positive definite* matrix-vector equation for $\boldsymbol{\lambda}$
- $\boldsymbol{u}$ and D are reconstructed within each element from the values of $\boldsymbol{\lambda}$ on the element edges.

Advantages: can implicitly include Coriolis term and avoid lumping the mass matrix.

Flux reconstruction

Solve the weak form of the mass continuity equation 4 in each element:

$$\int_e\phi\Delta D\,\mathrm{d}x-\Delta t\int_e\nabla\phi\cdot\boldsymbol{u}D\,\mathrm{d}x+\Delta t\int_{\partial e}\phi\tilde{D}\boldsymbol{u}\cdot\boldsymbol{n}\,\mathrm{d}s=0.$$

where $\tilde{D}$ is the value of D on the upwind side of ∂e, using standard DG advection methods - in this case, 3rd order SSPRK. **Aim:** to find mass flux $\boldsymbol{F}\in\mathbb{V}_1$ that satisfies $\Delta D=\Delta t\nabla\cdot\boldsymbol{F}$.
This mass flux can be constructed in each element by solving the following set of equations:

$$\int_{\delta e}\phi\boldsymbol{F}\cdot\boldsymbol{n}\,\mathrm{d}s=\int_{\delta e}\phi\tilde{D}\boldsymbol{u}\cdot\boldsymbol{n}\,\mathrm{d}S,\quad\int_e\nabla\phi\cdot\boldsymbol{F}\,\mathrm{d}x=\int_e\nabla\phi\cdot\boldsymbol{u}D\,\mathrm{d}V\quad\forall\phi\in\mathbb{V}_2,\quad\int_e\nabla^{\perp}\gamma\cdot\boldsymbol{F}\,\mathrm{d}V=0\quad\forall\gamma\in\mathbb{V}_0$$

Taylor-Galerkin methods for PV advection

Solve equation 6 using a multistage method with q at each stage defined as

$$\hat{qD}_i-\eta(\Delta t)^2((qD)_i)_{tt}=\Delta t\sum_{j=0}^{i-1}\mu_{ij}((qD)_j)_t+(\Delta t)^2\sum_{j=0}^{i-1}\nu_{ij}((qD)_j)_{tt}$$

where $i=1,...,k$ denotes the stage and the $\{\mu\}_{ij}$ and $\{\nu\}_{ij}$ are coefficients defined in [4].
Using equation 6 to replace temporal derivatives with spatial derivatives, we can write:

$$\int_\Omega\gamma\left((qD)_j\right)_t\mathrm{d}V=-\int_\Omega\nabla\gamma\cdot\boldsymbol{F}q\,\mathrm{d}V\qquad\text{and}\qquad\int_\Omega\gamma\left((qD)_j\right)_{tt}\mathrm{d}V=-\int_\Omega\frac{\boldsymbol{F}}{D}\cdot\nabla\gamma\boldsymbol{F}\cdot\nabla q\,\mathrm{d}V$$

which, comparing with equation 6, we see is exactly the form we require. We use a 2 level, 3rd order in time $\bar{T}(2,3)$ Taylor-Galerkin scheme to solve the continuity equation for q. This is stable for values of $\eta>0.473$.

Results

Solid body rotation:
Williamson [5], test case 2

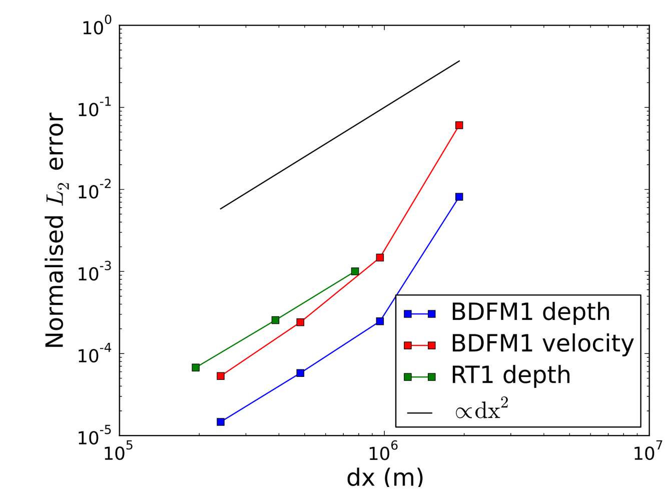

L^2 error of depth and velocity fields after 5 days, versus mesh size dx, for BDFM1 and RT1 finite element spaces.

Flow over mountain:
Williamson [5], test case 5

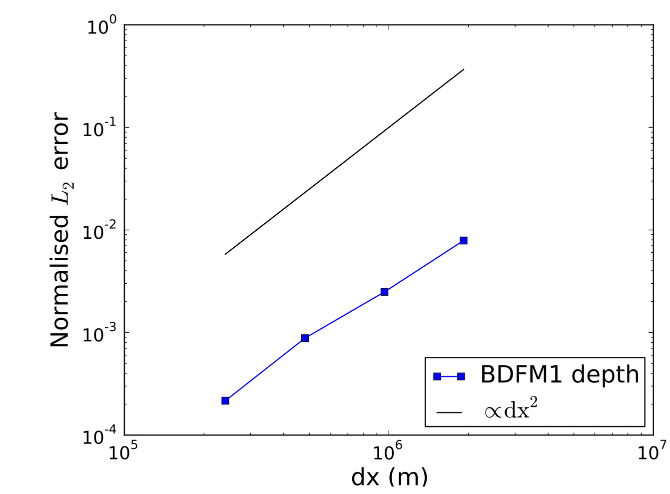

L^2 error of depth field, compared to reference solution, at 15 days, versus mesh size dx, for the BDFM1 finite element space.

Flow over mountain:
Snapshot of potential vorticity at 50 days for Williamson test case 5, for the BDFM1 finite element space.

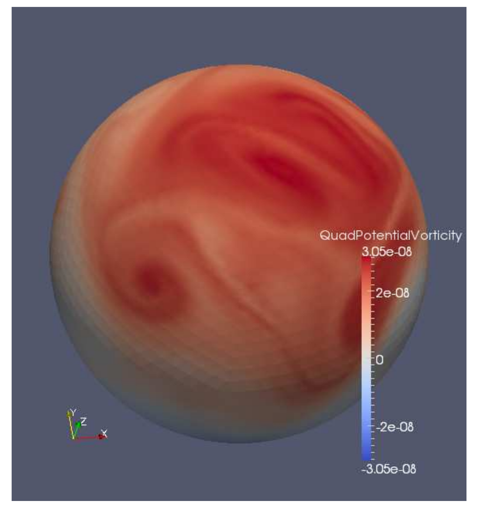

Barotropically unstable jet (Galewsky [2])
Vorticity field at 6 days for the barotropically unstable jet from Galewsky et. al. [2], using BDFM1 on a grid with 184320 DOFs, corresponding to an average mesh size of 240901m.

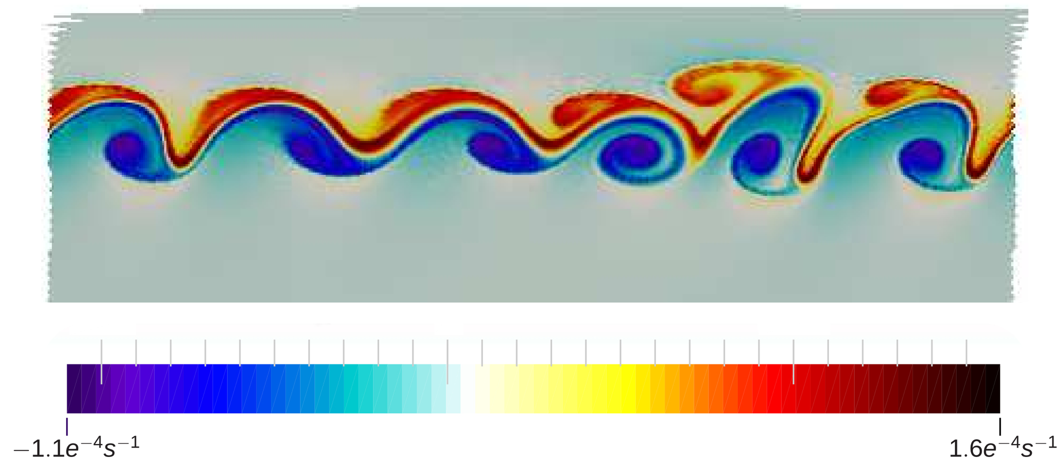

References

[1] CJ Cotter and J Shipton. Mixed finite elements for numerical weather prediction. *Journal of Computational Physics*, 231(21):7076–7091, 2012.
[2] Joseph Galewsky, Richard K Scott, and Lorenzo M Polvani. An initial-value problem for testing numerical models of the global shallow-water equations. *Tellus A*, 56(5):429–440, 2004.
[3] Andrew TT McRae and Colin J Cotter. Energy-and enstrophy-conserving schemes for the shallow-water equations, based on mimetic finite elements. *arXiv preprint arXiv:1305.4477*, 2013.
[4] A Safjan and JT Oden. High-order Taylor-Galerkin and adaptive h-p methods for second-order hyperbolic systems: Application to elastodynamics. *Computer Methods in Applied Mechanics and Engineering*, 103(1):187–230, 1993.
[5] David L Williamson, John B Drake, James J Hack, Rüdiger Jakob, and Paul N Swarztrauber. A standard test set for numerical approximations to the shallow water equations in spherical geometry. *Journal of Computational Physics*, 102(1):211–224, 1992.

Department of Mathematics, South Kensington Campus, Imperial College London, London, SW7 2AZ

Mail: `j.shipton@imperial.ac.uk`

website: `http://www.imperial.ac.uk/people/j.shipton`